International Journal of Scientific & Engineering Research, Volume 9, Issue 12, December-2018
ISSN 2229-5518

A proposed Automated System to Classify Diabetic Foot from Thermography

Marwa M. Eid, Reem N.Yousef, Mohamed A. Mohamed

Abstract— Diabetic foot is a major complication of diabetes mellitus worldwide. Early diagnosis and adequately treated is difficult by traditional methods. Previous studies revealed that thermography is a good monitoring tool for early detection of the diabetic foot. In this paper, a new proposed system will be introduced for the early diagnosis of the diabetic foot using thermal images and distinguishing among its four grades. The proposed system is based on combining textural and histogram features of thermal foot images and then classifying those using three different classifiers: (i) k-Nearest Neighbor; (ii) Support vector machine, and Decision tree. This proposed design provides an automatic classification of the diabetic foot using image analysis accurately in low elapsed time. Experimental results showed that Fine KNN has a maximum accuracy of 96.8%, a sensitivity of 88.3%, a specificity of 99.1%, and losses score of 0.004 using nine features only. When comparing the proposed system with the relevant systems, it's approved to be more accurate with low both elapsed time in learning and testing phase which can help the clinicians in the simply automatic diagnosis of the diabetic foot and distinguishing between them.

Index Terms— DF, DT, Diabetes mellitus, Early diagnosis, KNN, SVM, Thermal imaging

———————————— u ————————————

1 INTRODUCTION

Nowadays, Detection of the diabetic foot (DF) using thermal images is one of the most important research areas in the medical field. Because of the rapidly increasing number of diabetic patients, which scored 194 millions in 2004 and this value is expected to reach 439 millions in 2030 [1]. One of the risk factors for this disease is foot complications especially at the advanced stages of the disease. Most diabetic patients suffer from diabetic foot ulcers, these ulcers, if not treated rapidly, may lead to partial or total amputation. The DF ulcers can be prevented by early detection and treatment. It's almost impossible to early detect diabetic foot ulcer using traditional methods for diagnosis. There are also difficulties in self-examination, because of gradual loss of sensation of the patients. Also, there isn't an automated system for early detection of ulcers. Previous studies showed that there is a relationship between increase in temperature and diabetic foot ulcers appearance [2]. There are various algorithms that can be used for early diagnosis of diabetic foot ulcers using temperature assessment such as infrared images [3-7], liquid crystal thermography (LCT) [8], infrared (IR) thermometer and temperature sensors integrated into a weighing scale [8].

In this paper, the main concern is to distinguish between healthy and diabetic foot ulcers. Another important concern is to identify a type of DFs' using thermal statistical and image analysis. In the proposed automated system, thermal images are acquired using FLIR-ONE thermal camera which is connected to an Android based smartphone. The thermal feet images are then analyzed using two categories of digital image processing techniques: (i) classical thermal statistics and (ii) proposed image analysis. Classical thermal statistics can be achieved by measure regions of interest (ROI) points in both feet using FLIR tools software and compute the absolute temperature difference between them. Unfortunatly, this method is not accurate because of changes in foot temperature and identifies all cases of diabetes using it is difficult owing to it lacks of information about the shape and size. The proposed image processing system by getting rid of noises from thermal images such as shifting, unwanted clothes, and malleolus bone. Then isolate feet from the background and extract its features. Finally, the extracted features are classified using different classifiers. As a result of building k-Nearest Neighbor (KNN) based classifiers, the largest accuracy will be achieved by concatenating fusion between textural and histogram features. Thus, the proposed system outperforms the classical thermal statistics in distinguishing between diabetic foot cases automatically with high accuracy.

The rest of the paper proceeds as follows: section-2 provides a description of the related work of DF thermal images; Section-3 explains materials and methods of the proposed data acquisition system, section-4 presents the details of the proposed system, section-5 introduces and discusses the simulation results, section-6 provides conclusions and future works.

· *Reem yousef is a teaching assistant in Delta Higher Institute for Engineering and Technology.*
· *Marwa Eid is a teacher in Delta Higher Institute for Engineering and Technology.*
· *Mohamed A Mohamed is a Professor and head of the Department of Electronics and Communication Engineering in faculty of engineering, Mansoura University.*

2 Related Works

There are many researches that focused on the diagnosis of diabetic foot diseases using thermal images by measuring skin temperature variation. Thermal foot images have been used to differentiate between diabetic foot with and without sympathetic skin response by P. Sun et al. at [3]. This can be achieved by; dividing images into six ROI regions arch, heel, Forehead, Lateral Sole, Hallux, and Lesser Toes.Then compute the mean temperature difference to compare them with healthy participant's temperature. G. Serbu [4] proposed a system that can diagnose a diabetic foot using thermal images by computing the temperature of corresponding points in both feet. The result declared that the average temperature in neuropathy patients ranged between 32.8 and 27.9 ºC. C. Liu et al. [1] presented a system to detect diabetic foot ulcer by applying image processing on thermal images. Segmentation, registration, and abnormality detection are the steps of this technique. Segmentation was done using active contour to extract the foot from the background and registeration was done using B-spline non-rigid registration to align both feet in the same position. Finally, the detection of abnormality was done by subtraction the intensity level of corresponding areas in the left and right foot. Regarding this study, if the temperatures difference is more than threshold, it refers to an abnormal area. J. Netten et al. [5] have been used infrared images in differentiating among three categories of diabetic foot as the following; no visible sign, local, and diffuse complications. This can be achieved by calculation the mean temperature difference between the ipsilateral and the contralateral foot. H.Peregrina-Barreto et al. [6] detected the abnormality of the diabetic foot using thermal image by associating between the area temperature and its color code. In this method, they used a rainbow palette, then segments it into ten colors the difference between each one 1◎. L. Fraiwan et al. [2] proposed a thermal system using an Android smartphone and MATLAB Mobile platform. This system can predict ulcers from four different ROI areas by comparing them with the normal test image. However, the cases that were at high risk of complication were not declared in the study and the only focus was on the prediction of ulcer in grade zero diabetic foot with depending on statically thermal values. Infrared images are used in [7] to detect the diabetic foot by applying image processing. Morever, this system achieved the largest accuracy 95.66%. However, this study was just interested in detection of abnormalities only. M. Goyal et al. [9] were able to classification diabetic foot ulcers only using a different convolutional neural network. M. Adam et al. [10] proposed a thermal system based on extracting textural and entropy features from decomposed discrete wavelet transform (DWT) and higher order spectra (HOS) to detect the abnormality of the diabetic foot. Unfortunately, this study can't detect diabetic foot type just; it could detect the abnormality with identification rate 89.39%.

3 Materials and Methods

The proposed system has two main parts: hardware and software. The hardware consists of infrared camera and android smart phone. On the other hand, the software consists of FLIR Tools + 5.13 (5.13.17214.2001), Microsoft Excel program, and MATLAB 2017b.

3.1 Acquisition Protocol

The thermal acquisition system consists of FLIR ONE thermal camera, Samsung Note five smartphone, temperature and humidity sensor, tripod, Polyurethane foam, and Accu-Chek Active meter. Materials of data acquisition system are shown in Fig. 1.

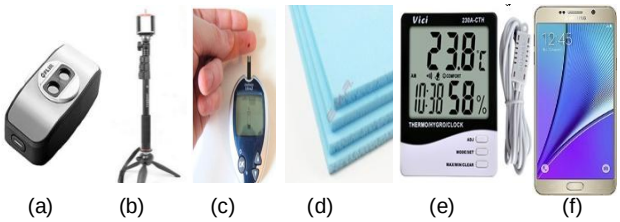

Fig. 1 materials of data acquistion system (a) FLIR ONE, (b) tripod, (c) Accu-Chek Active meter, (d) Polyurethane foam, (e) sensor, (f) Samsung Note 5.

Each material in acquisition system had a unique usage. Such as Tripod for fixing camera, Accu-Chek Active meter for measuring suger level, Polyurethane foam for isolating feet from whole body, sensor for measuring temperature and humidity value. The thermal acquisition system also contains: FLIR ONE thermal camera which has two lenses; lepton and standard [2]. There are a lot of specific properties of this camera that should be considered before image analysis: sensitivity, temperature range, resolution, and field of view as tabulated in Table 1 [2].

Table1

FLIR ONE Thermal Camera Specifications

Camera specification	Value
Temperature Measurement Range	-20° to 120°C
Field Of View (FOV) H×V	46 × 35 °
Detector Resolution	160 × 120 pixel
Thermal Sensitivity	0.1 ℃.

3.2 Methods and Conditions

To acquire thermal foot images, the following steps will be applied:

Step (1): connect infrared camera with smartphone.

Step (2): support them by a tripod to keep it in a fixed position in all cases with 60 cm distance away from the patient's feet.

Step (3): measure the room temperature and humidity to ensure the room temperature within a range from 18 to 23℃ and humidity (< 50%).

Step (4): maintain patients with barefoot at least for 10 minutes in this atmosphere.

The patient should put his\her foot in polyurethane foam which has two holes in its center to ensure that all thermal images are in the center field of view thermal camera to obtain homogenous background; the proposed data acquisition system is shown in Fig. 2. The next step is recording the acquired data of each patient in Microsoft Excel worksheet: age, gender, body mass index (BMI), and blood sugar level (BSL).

Fig.2 the proposed data acquisition system

3.3 The Aquired Dataset

The diabetic feet can be classified into four grades [1]. The difference between each grade and the other is in shape, size, and variance in colors between both feet. For instance, in grade zero there is variance between corresponding ROI points and in grade one there is a superficial ulcer and also variance in colors between corresponding ROI points While in grade two there is deep ulcer which called infected ulcer or Charcot's foot and in grade 3 there is any amputation in feet due to diabetes. A convenience sample of 50 subjects has participated in this proposed system.

The participated has been selected from healthy and diabetic patients of the Neuropathic Foot Clinic at Dar el shefaa Hospital, Dakahlia Governorate, Egypt. The acquired database contains 500 images which are divided equally into five groups and each group contain 10 cases as follows: (i) the patients without any signs of complications (grade 0), (ii) the patients with local signs of complications (e.g., superficial ulcer) (grade 1), (iii) the patients with deep complications (e.g., deep ulcer reached to tendon or Charcot's foot) (grade 2), (iv) the patients with amputation (grade 3), and (vi) the healthy volunteers (normal).A sample of natural RGB and thermal sample image are shown in Fig. 3. There aren't variances in colors between both feet in Fig. 3a which refers to a normal case, but there are variances in colors between both feet in Fig 3b which refers to grade 0 DF, right foot appears in green color but left foot appears in red color or right foot is colder than left foot.Moreover, there is a superficial ulcer in left foot in Fig 3c so this case refers to grade 1 DF, and there is a deep ulcer in right foot in Fig 3d so this case refers to grade 2 DF. Finally, all right toes amputated in Fig 3e, thus, it refers to grade 3 DF.

3.4 Classical Thermal Image Analysis

In the proposed system, thermal image analyses go through the following steps:

Step (1): measure the temperature of nine ROI regions 1st, 3rd and 5th toe, 1st, 3rd and 5th distal metatarsal, 1st and 2nd lateral and heel points in right and left feet using FLIR Tools software, as shown in Fig. 4.

Step (2): record the results in excel worksheet.

Step (3): compute mean absolute temperature difference between corresponding points in both feet.

In case there is no temperature difference (ΔT) >1.5 °C between two feet's this refer to normal case, ΔT >1.5 °C refer to grade zero, ΔT >2 °C refer to grade one, ΔT >3 °C refer to grade two and in case there is amputation this refer to grade three diabetic foot [5].

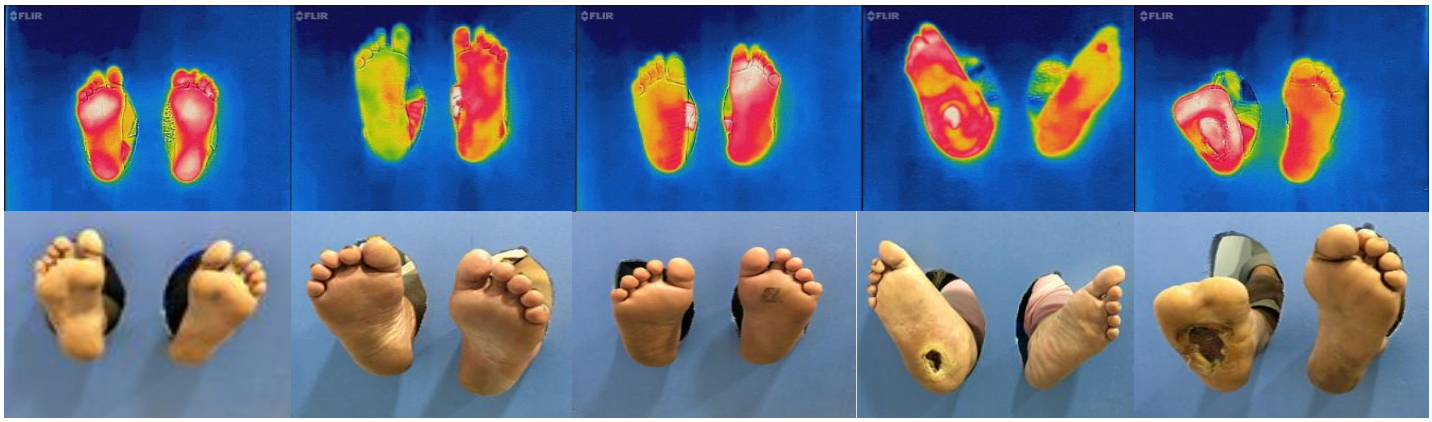

(a) (b) (c) (d) (e)

Fig. 3 Thermal and visual images (a) normal, (b) grade0, (c) grade 1, (d) grade2, (e) grade 3.

The main drawback in diagnosis by this method is the lack of accuracy owing to its critical needing for a professional specialist. Moreover, the fatal errors which might result in diagnosis could increase the probability of errors due to manual selecting ROI points and lacking information about the shape and size.

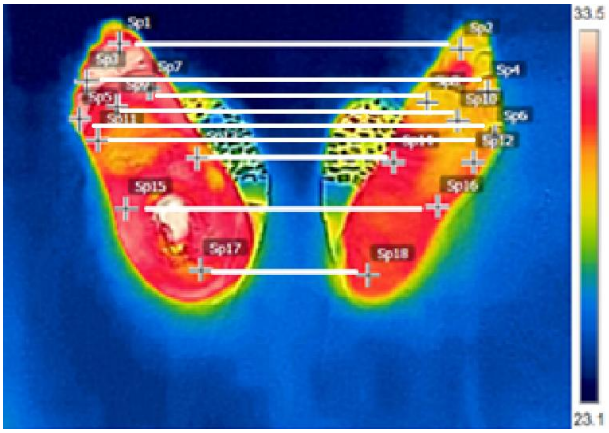

Fig.4 Thermal image temperatures results from FLIR TOOLS

4 The Proposed System

As an alternative to thermal analysis, MATLAB image processing toolbox is preferred to be used. The acquired thermal images are analyzed as shown in Fig. 5. The proposed system passing through steps could be described as:

Step (1): preprocessing to remove malleolus bone and other noise from gray thermal images.

Step (2): segmentation to isolate feet from a background and then fit them in the same size and position.

Step (3): feature extraction to select main features from images depending on the natures of different diseases.

Step (4): feature fusion to combine among features.

Step (5): classification to identify each class.

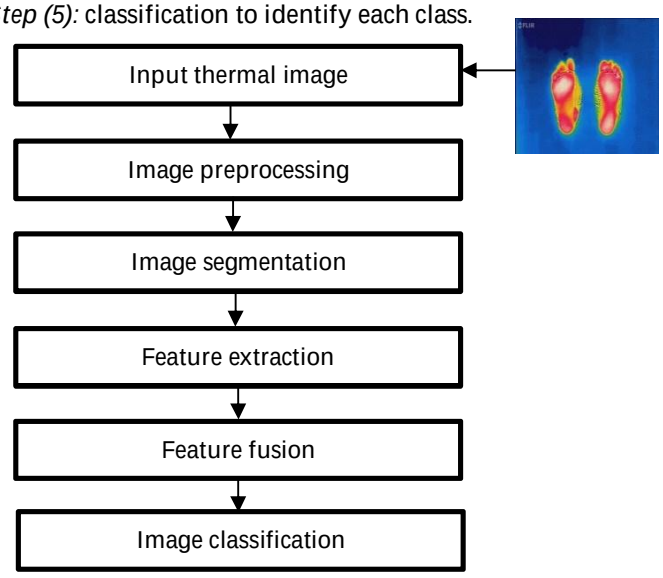

Fig. 5 Thermal image analysis steps.

4.1 Image Preprocessing

In the input thermal images with resolution 480×640 pixels, there are many noises which are related to change in patient feet position, shifting, rotation, malleolus bone, and unwanted clothes. These noises result from motion patient feet during data acquisition system. In case of not getting rid of these noises, this may dramatically affect the system performance and decrease the classification accuracy. Thus, the aim of pre-processing is to remove the mentioned noises and focus on acquired feet (ROI) only. For instance, Fig 6 refers to samples of noises in the dataset, Fig 6a the malleolus bone disturbance, Fig. 6b unwanted clothes, Fig 6c large distance between two feet's and Fig 6d rotation of one foot. All the mentioned noises should be eliminated before feature extraction stage.

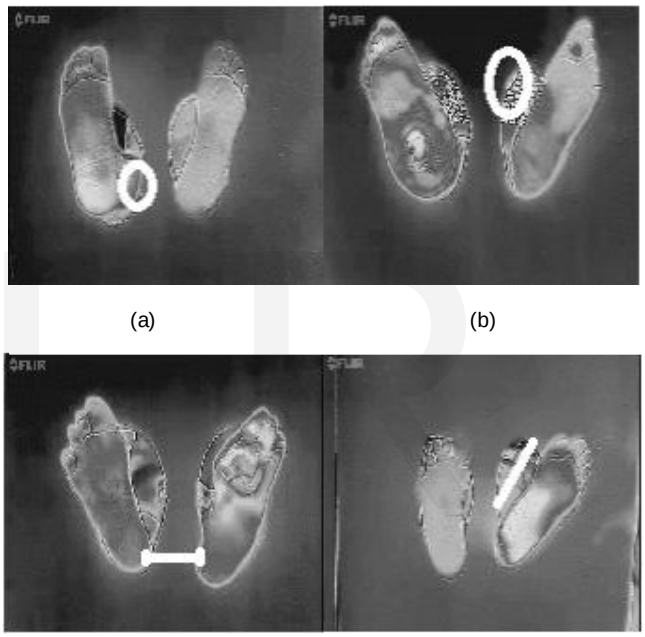

Fig.6 Example of noises in dataset thermal image, (a) malleolus bone disturbance, (b) unwanted clothes, (c) large distance between both feet's and (d) rotation.

The proposed preprocessing system is summarized in seven steps are involved:

Step (1): converting all thermal images to gray scale.

Step (2): creating feet mask using Gaussian Otsu threshold.

Step (3): filling mask holes.

Step (4): applying active contour on mask.

Step (5): isolating feet from background by subtracting gray scale image from mask.

Step (6): eroding segmented images.

Step (7): using geometric transformation to normalized and centralized them.

In the previous steps, convert thermal images to gray scale to simplify segmentation process and reduce the elapsed time, A Gaussian Otsu threshold [11] is then applied on the gray scale image to automatically create a feet mask and fill this mask based on morphological reconstruction [12]. Active contour [13] is used to smooth the mask edges by 500 iterations using trial and error method. Subtract the generated mask from original gray scale to obtain the isolated feet with a homogenous background then using morphological eroding operation [14] to remove noises from edges which result from subtraction. Finally, use geometric transformation such as crop, rotation and translation to normalize and centralize all isolated images in the same position with the same size. All images after segmentation became 380 × 450 pixels; flow chart of the proposed preprocessing technique is shown in Fig. 7, the main steps of applying it to a sample gray scale thermal image is shown in Fig. 8. Sample of the preprocessing results are presented in Fig. 9, from the figure easily could be preserved that the areas of ROI i.e. feet areas had been isolated correctly and disposed of all related noise accurately.

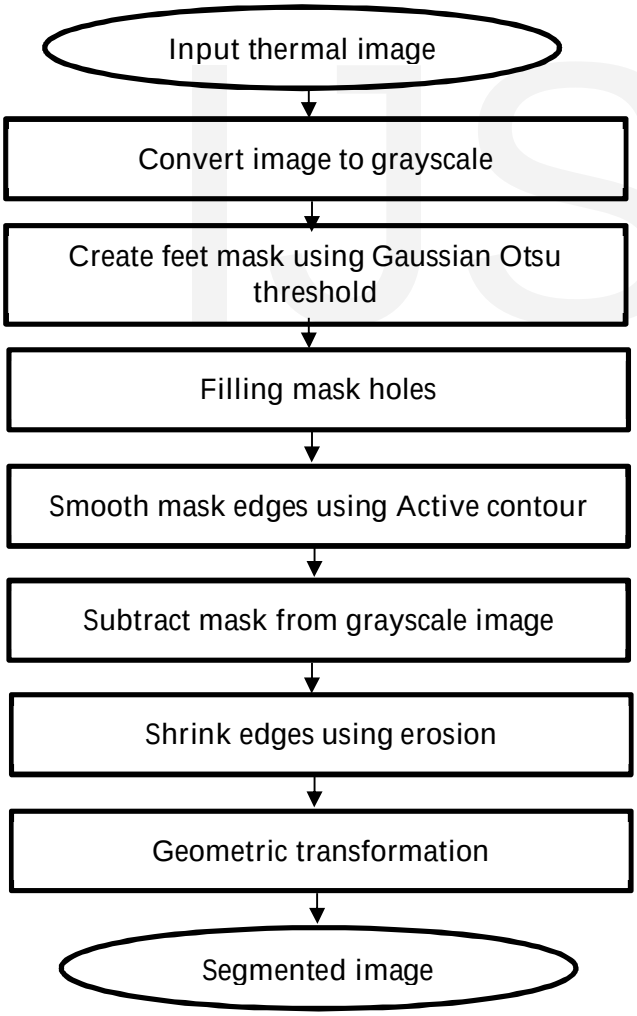

Fig.7 Flow chart of the proposed preprocessing system

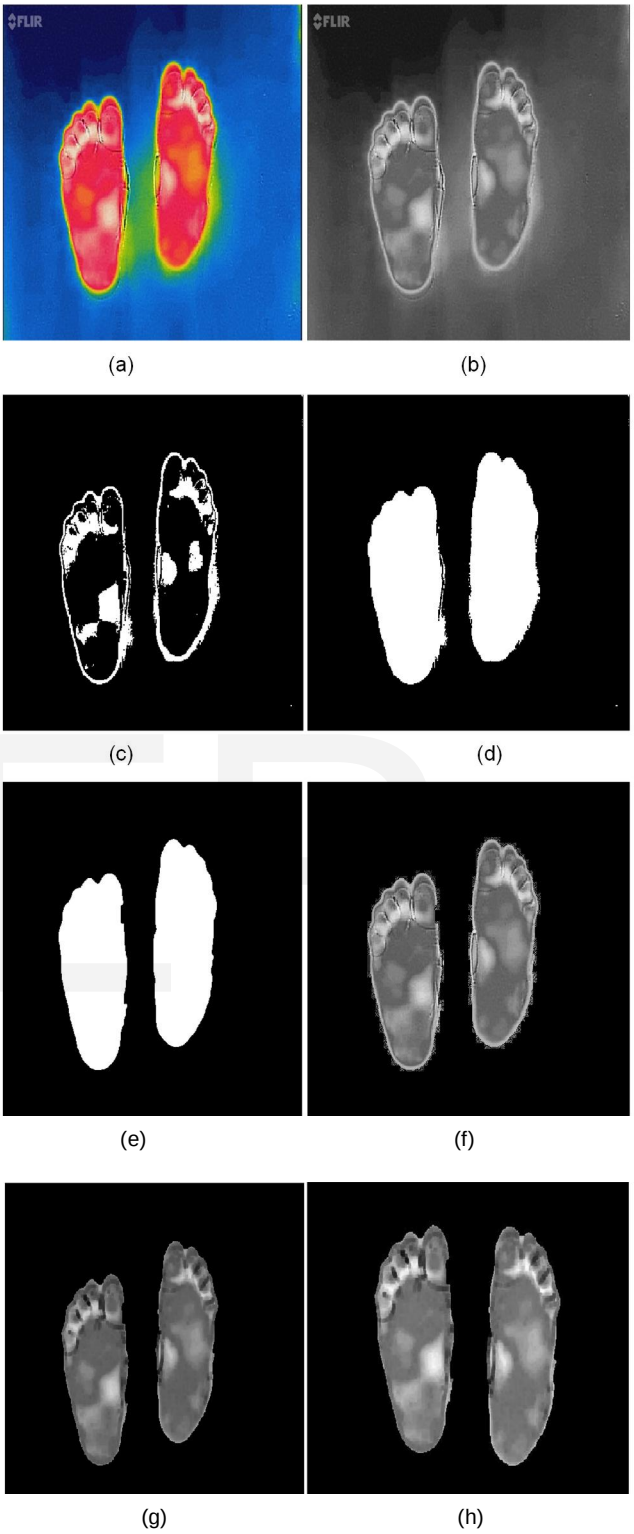

Fig. 8 Sample of the preprocessing stage results, (a) thermal image, (b) gray scale image, (c) Results of Gaussian Otsu image, (d) filling mask, (e) active contour mask image, (f) gray scale after subtraction, (g) erode image, and (h) segmented image.

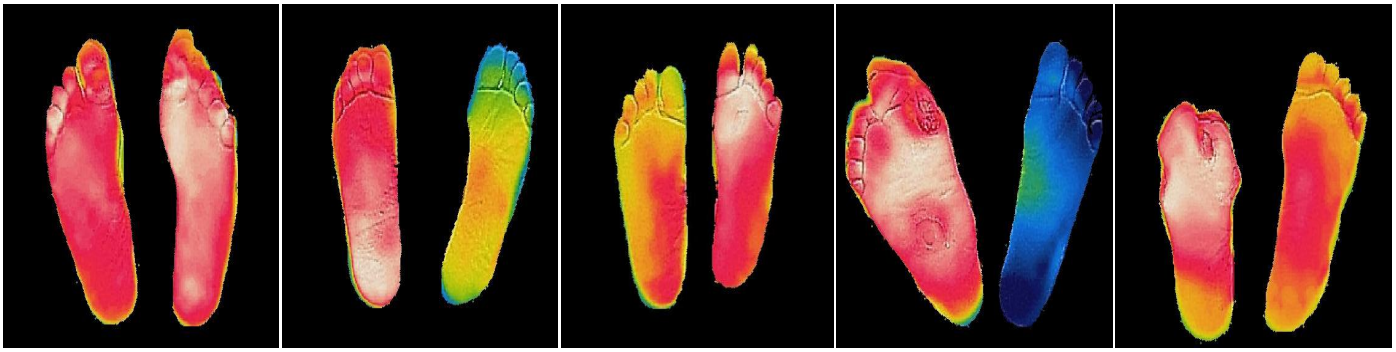

(a) (b) (c) (d) (e)

Fig. 9 Sample segmented images,(a) normal, (b) grade 0, (c) grade 1, (d) grade 2, (e) grade 3

4.2 Feature Extraction

Feature extraction starts from a set of image data and extracting main features from it, which intended to facilities learning, informative and non-redundant. There are different methods of feature extraction techniques like spatial and transformed feature extraction. Spatial features such as Surf, Harris, Fast, textural and histogram features, but transformed features such as wavelet transforms, discrete cosine transform, Fanbeam, Radon, principle component analysis (PCA) and histogram of gradient (HOG) [15]. The differences among diabetic feet patient's cases belong to irregularity or deformation in feet shape, Change in size of one of them and the missing contrast in colors between both feet for instance. In grade 0 there is variance in corresponding areas colors, in grade 1 there is a superficial ulcer, in grade 2 there is a deep ulcer or Charcot's foot, in this case, one of the feet's bigger than the other one and in grade 3 there is amputation in ROI one of them or both. In this paper, textural and histogram features are extracted.

Textural Features

Textural features are extracted from the gray level co-occurrence matrix (GLCM) which represent a square matrix with size L*L [15], where L indicates a number of grey-level in the original image. GLCM contains the probability value of two pixels with i and j grey-level intensity, respectively, which is separated by distance d and direction θ, and the probability value is $P(i,j,d,\theta)$. There is some statistical measurement extracted from GLCM which refer to texture features such as homogeneity, contrast, moment, and correlation. Hence the size of the feature vector for one patient image is 1×4. Contrast measures variation in the gray level of an image, thus a smooth image have a low value of contrast and otherwise in a coarse image. Contrast is calculated by [15],

$$\text{Cont} = \sum_{i,j=0}^{L-1} (i-j)^2 . P(i,j,d,\theta) \quad (1)$$

where, i and j grey level intensity, d is a separation distance, θ is a direction, and $P(i,j,d,\theta)$ is the probability value

Homogeneity is called Inverse Difference Moment (IDM) and it's inversely proportional to contrast. IDM is calculated by [15],

$$\text{IDM} = \sum_{i,j=0}^{L-1} \frac{P(i,j,d,\theta)}{i + |i-j|^2} \quad (2)$$

Energy is called the second moment and measure uniformity; a homogenous image has a high value of energy. Energy is calculated by [15],

$$\text{Energy} = \sum_{i,j=0}^{L-1} P^2(i,j,d,\theta) \quad (3)$$

Correlation measures the linearity between two pixels. Correlation is calculated by [15],

$$\text{corr} = \sum_{i,j=0}^{L-1} \frac{(i-\mu_x)(j-\mu_y)P(i,j,d,\theta)}{\sigma_x \sigma_y} \quad (4)$$

where, $\mu_x = \sum_{i,j=0}^{L-1} i . P(i,j,d,\theta)$, $\mu_y = \sum_{i,j=0}^{L-1} j . P(i,j,d,\theta)$, $\sigma_x = \sum_{i,j=0}^{L-1} (i-\mu_x)^2 . P(i,j,d,\theta)$, and $\sigma_y = \sum_{i,j=0}^{L-1} (i-\mu_y)^2 . P(i,j,d,\theta)$

Histogram Features

A histogram is the plot of intensity values in images which give information about image natures [16].

There are features extracted from histogram plots such as mean, variance, entropy, skewness and kurtosis. So the size of the feature vector for one patient image is 1×5.

Mean is the average value and refer to image brightness, the bright image has a high value of mean which calculated by [16],

$$\tilde{g} = \sum_{g=0}^{L-1} gP(g) \quad (5)$$

where, g is the gray level, L is the intensity level equal 256 and P (g) is the probability distribution of all pixel values.

Variance is proportional to contrast; the high value of contrast gives a high value of variance and otherwise. Variance is calculated by [16],

$$\sigma = \sum_{g=0}^{L-1} (g - \tilde{g})^2 P(g) \quad (6)$$

where, g is the gray level, $\tilde{g}$ is the mean value, L is the intensity level equal 256 and P (g) is the probability distribution of all pixel values.

Entropy measures numbers of bits which needed to code image data and calculated by [16],

$$\text{Entropy} = -\sum_{g=0}^{L-1} P(g)\log_2[P(g)] \quad (7)$$

where, g is the gray level, L is the intensity level equal 256 and P (g) is the probability distribution of all pixel values.

Skewness measures the mean intensity asymmetry distribution and calculated by [16],

$$\text{Skew} = \frac{1}{\sigma_g^3} \sum_{g=0}^{L-1} (g - \tilde{g})^3 P(g) \quad (8)$$

where, g is the gray level, $\tilde{g}$ is the mean value, L is the intensity level equal 256 and P (g) is the probability distribution of all pixel values.

4.3 Feature Fusion

Fusion is the process of merging multiple input images into a single informative output image. Multi-sensor fusion is used to achieve high spatial and spectral resolutions by combining features from different sources of information [17]. The resulting features will be more informative than the input images. There are several methods of feature fusion such as High pass filtering, Intensity Hue Saturation transform (IHS), PCA, Wavelet Transform (WT), Laplacian pyramids, Discrete Cosine Transform (DCT), and concatenating fusion. In this paper, concatenating fusion will be employed to combine textural and histogram features to reduce system complexity and the elapsed time in addition to replace or repair the defect of image data, improves the spatial resolution, and the geometric precision. As the length of a textural feature vector is 1×4 and histogram feature vector 1×5, thus the result fused feature vector will be 1×9 length which then classified using different classifiers.

4.4 Image Classification

K- nearest neighbor (KNN)

In 1970's, KNN is used in statistical applications because it depends on calibration dataset [15]. In KNN the image is identified by comparing it with training images set using a distance metric [18]. Thus, in case of low distance, the test image is belongs to the training set. The distance function is considered a basic function of KNN and the Euclidean distance between two points is the most commonly used one which calculated by [18],

$$\text{dist}(X_1, X_2) = \sqrt{\sum_{i=1}^{n} (x_{1i} - x_{2i})^2} \quad (9)$$

where,

$X_1 = (x_{11}, x_{12}, \ldots, x_{1n})$ and $X_2 = (x_{11}, x_{12}, \ldots, x_{1n})$

The steps of classification learning using KNN is summarized by (i) compute the distance between new training image and all sample images, using distance function, (ii) find k sample which is close to unknown samples in distance (iii) compute the value of unknown samples by calculating the average value of the response value from k samples [18]. The k value is considered a tuning parameter in small value of k the algorithm will have low bias and high variance. The decision boundary in this case graphically appeared jagged. In the case of the large value of k, the decision boundaries will be smoother and this means that high bias and low variance. The value of k can be calculated by using bootstrapping procedure which relies on random sampling with replacement [19].

Support Vector Machine (SVM)

Support vector machine (SVM) for classification is a supervised learning which can construct a single hyper-plane or many of them to separate between classes. In addition to this method, it also searches for a margin to achieve the largest distance to the nearest training data [19]. The basis function in SVM is the kernel function which can be transformed nonlinear spaces to linear ones. There is also nonlinear package such as polynomial and sigmoid functions [20]. The user just selects the appropriate kernel function then the software transforming the data and classifying it, polynomial and radial basis functions are commonly used in case of a large dataset. Gaussian kernel function is calculated by [20]:

$$k(x, y) = \exp(-\gamma * (x - y)^2) \quad (10)$$

Where: γ refer to the value of gamma.

Gamma is a positive scalar value which refers to kernel scale value which exerted on kernel function. If the value of gamma is large, this means that the separation between x and y large else otherwise. Gamma value is related to how to spread out the features matrix.

Classification images using SVM by (I) plot each feature as a point in n-dimensional space and (II) search for a hyper-plane that separates two classes well. Example of two classes separating by a hyper-plane is shown in Fig. 10 [18].

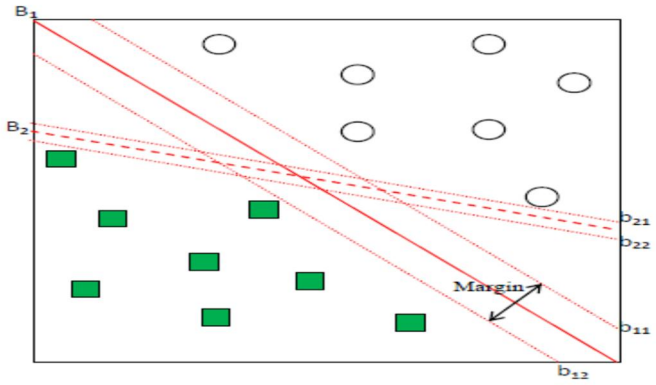

Fig.10 example of two classes separating by hyper-plane

Decision Tree (DT)

Decision tree (DT) structure is like the natural tree, each node of this tree refers to a test sample, each node refers to the output of test sample, and each leaf refers to class label. During the construction of this tree, the decision tree splits each node and selects the best split which improves the classification accuracy. The other function of selection is pruning the tree to remove the branches which hold noise [18] and prevent overfitting, the structure of decision tree is shown in Fig. 11.

The selection of splitting depends on four different algorithms: Gini Index, Chi-square, Gain and Gain Ratio [18]. The most common of these algorithms are the Gini Index which proportional to the homogeneity. So, in case of the high value of Gini, the homogeneity also becomes high which performs binary splits only. There are impurities in the training subsets which come from generating decision tree but the Gini index can minimize it, the Gini index is calculated by [20],

$$G(C|A_{ij}) = 1 - \sum_{k=1}^{J} p^2(C_k|A_{ij}) \qquad (11)$$

Where A_i is the attribute used to branch the tree, J is the number of classes in our classification problem.

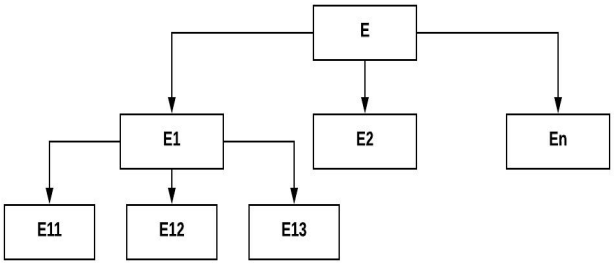

Fig.11 structure of decision tree

5 Results And Discussion

In the proposed system, when employing textural and histogram features to the mentioned classifiers. The largest overall accuracy is achieved from Fine KNN classifier which scored 96.8% classification accuracy using five cross validations, one nearest neighbor and Euclidean distance metric. The accuracy results are shown in Fig. 12.

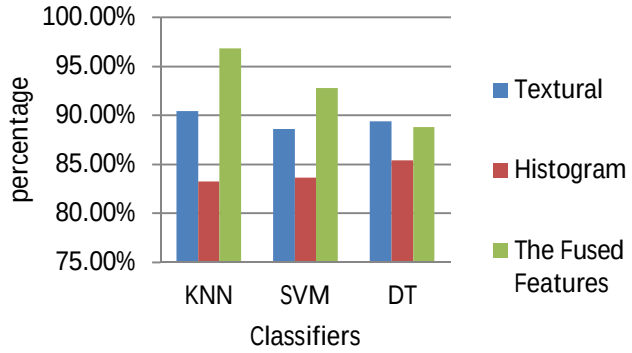

Fig.12 accuracy results of classifiers

The results of accuracy presented in Fig. 10 proved that KNN on the fused feature vector between textural and histograms features outperform other classifiers. The detailed accuracy of KNN is tabulated in Table 2. Sensitivity, false positive rate, precision, and F-score are used to evaluate the performance of the proposed system. They are defined as follows:

Sensitivity is the true positive rate (TPR) which measures the portions that are correctly classified, it is calculated by [21]:

$$TPR = \frac{TP}{TP + FN} \times 100 \qquad (12)$$

where, TP is true positive value and FN is false negative value.

False positive rate (FPR) is the fall-out value which measures of incorrectly portions, it can be defined as [21]:

$$FPR = \frac{FP}{FP + TN} \times 100 \qquad (13)$$

where, TN is true negative value and FP is false positive value.

Precision is referring to positive predictive value (PPV) where it measures true positive value against positive value, it can be defined as [21]:

$$PPV = \frac{TP}{TP + FP} \times 100 \qquad (14)$$

F-score is measures a harmonic mean of precision and recall, it can be calculated by [21],

$$F - score = \frac{2TP}{2TP + FP + FN} \times 100 \qquad (15)$$

From confusion matrix, there are important variable should be extracted; True Positive (TP), True Negative (TN), False Positive (FP), False Negative (FN), False Discovery Rate (FDR) and False Predictive Rate (FPR). Fig.13. refers to the confusion matrix of the fused features by Fine KNN classifier.

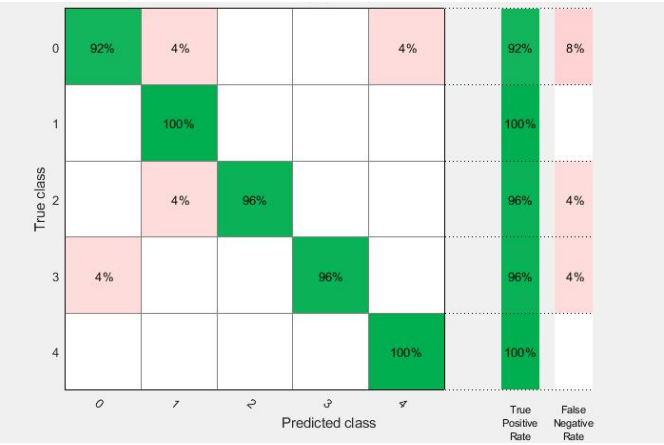

Fig.13 confusion matrix (Fine KNN)

The detailed accuracy of the fused features using Fine KNN classification by the classes of fifth class of diabetes is tabulated in Table 2. The patient classes are normal, grade 0, grade 1, grade 2, and grade 3.

Table 2 refers to identification of diabetic foot disease when integrating textural and histogram features to obtain whole statistical features. The value of accuracy is 96.8%, sensitivity is 88.3%, specificity is 99.1%, losses value is 0.0040, AUC is 0.972, FNR is 3.2%, and the Elapsed time is 0.61233 sec by using Euclidean distance. When textural and histogram features have been combined, the accuracy value enhanced by 7.07%, 16.3 % over using textural and histogram separately respectively. To measure the proposed system performance, its overall accuracy has been compared with SVM and DT. The results showed that the largest accuracy had been achieved by KNN owing to its effectiveness in distinguishing among statistical features which differ from case to other. When the combining textural and histogram are classified using KNN, the classification accuracy enhanced by 4.3%, 9% over using SVM and DT respectively. For Further confirmation, in Table 3, the methodology, accuracy, sensitivity, and specificity of studies on temperature distribution analysis and the proposed system are tabulated.

Table 2

Detailed Accuracy of the fused features by Fine KNN classifier

Class	Accuracy	TPR	TNR	FPR	Precision	F-score	AUC
Normal	96.8	88.4	98.9	1.01	95.83	92	93
Grade 0	96.8	92.5	97.9	2.04	92.5	92.5	99
Grade 1	96.8	85.7	100	0	100	92.3	95
Grade 2	96.8	85.7	100	0	100	92.3	100
Grade 3	96.8	89.2	98.9	1.03	96.1	92.5	99
Average	96.8	88.3	99.1	0.81	96.9	92.3	97.2

Table 3

Performance parameters of studies on temperature distribution analysis

Reference (year)	Methodology	Accuracy	Sensitivity	Specificity
Oe et al. (2013) [22]	· MRI scans · Infrared imaging · Ankle-brachial index (ABI) · Toe-brachial index (TBI) · Nerve conduction velocity · SPSS for statistical analysis	Undefined	60%	100%
Van Netten et al. (2014) [23]	· Infrared imaging · Compute average temperature of six sub regions on feet · Calculate the area under the receiver operating characteristic curve · Analyze Mean temperature difference by the Kruskal–Wallis tests.	Undefined	89%	78%

Hernandez-Contreras et al. (2015) [24]	· Infrared imaging · Grayscale characterization · Arch segmentation based on histogram distribution · Mathematical morphology	88.05% (normal) 94.33% (diabetic)	Undefined	Undefined
Purnima et al. (2017) [7]	· Thermal imaging · Image preprocessing · Foot segmentation · Feature extraction · Images classification by KNN, PNN, SVM	95.66% (KNN) 61.18% (PNN) 75.13% (SVM)	84.49% (KNN) 61.26% (PNN) 86.8% (SVM)	96.44% (KNN) 61.04% (PNN) 61.93% (SVM)
Goyal et al. (2017) [9]	· Thermal imaging · Feature extraction · Diabetic foot ulcer classification · Novel Convolutional Neural Network	92.5%	93.4%	91.1%
Adam et al. (2018) [10]	· Infrared imaging · Feet segmentation · Feature extraction · Image Classification by SVM	89.39%	81.81%	96.97%
Vardasca et al. (2018) [25]	· Infrared imaging · Localization and extraction · Identification of ROI · Classification using KNN and Weka.	92.5% (KNN) 93.4% (Weka)	Unidentified	Unidentified
The Proposed System	· Thermal imaging · Image preprocessing · Feature extraction · Feature fusion · Image classification	96.8%	88.3%	99.1%

By comparing the results of the proposed system results with both the results of thermal statistics results and medical diagnosis, the same medical diagnosis identically obtained. Moreover, the proposed system could offer the medical diagnosis results automatically with high accuracy and fast testing mechanism also it reduce spontaneous errors due to less human interventions. Thus, it could be more attractive to clinicians because of its ability of diagnosis and detection of diabetic foot type quickly, accurately and simply. From Table 3, the result of classification accuracy has been enhanced by 1.2%, 3.6% than the system in [7], and [25] respectively. The reason for increasing classification accuracy is combining textural and histogram features instead of using textural features only. Accuracy and specificity have been enhanced by 4.6% and 8.7% than the largest convolutional neural network used in [9] but the sensitivity is decreased by 5.7%. In the proposed system, accuracy, sensitivity, and specificity have been enhanced by 8.3%, 7.9%, and 2.19% than a system in [10], because of using only five statistical features and test them using support vector machine. The sensitivity has been enhanced by 47.1% but the specificity has been decreased by 0.9% than the system in [22] and the specificity has been enhanced by 27% but the sensitivity has been decreased by 0.79% than the system in [23]. The advantages of the proposed methodology are given below: (i) the proposed system obtained clear thermal feet patterns for the five classes of normal and DF automatically as shown in Fig. 9, (ii) it automatically distinguish among DF classes, (iii) it is accurate, easy, and simple, and (iv) it acquired maximum accuracy of 96.8%, sensitivity of 88.3%, and specificity 99.1%. Thus, the proposed method is fast as it used texture and histogram features to achieve the highest performance. On the other hand, the limitations of the proposed system include: (i) it is used only 50 subjects, (ii) the classification using machine learning needs extract featuires, (iii) IR thermography is expensive, and (iv) IR thermography needs special conditions.

6 CONCLUSIONS

This paper presents a new technique for automatic diagnosis of DF. Due to the alarming rate of the spread of this disease around the world, particularly in poor countries, encourages medical professionals to search for new strategies for an automatic and early diagnosis to avoid its devasting consequence. It's notable that traditional methods of diagnosis are not effective which lack important information about the shape and size of feet. The latest studies revealed that the thermography is a good monitoring tool of diagnosis which can see the variation in feet temperature. In the proposed system, the database of 500 thermal feet images has been acquired in special circumstances from 50 volunteers divided into five classes. Textural and histogram features are extracted from the segmented feet images for further analysis. SVM, DT, and KNN are used for verifying the classification accuracy. When comparing the performance of the three classifiers, the KNN had reached the most efficiency with maximum classification accuracy, which enhanced the classification accuracy by 4.3%, 9% over using SVM and DT respectively. The proposed system achieved a maximum classification accuracy of 96.8%, a sensitivity of 88.3%, and a specificity of 99.1% using only nine

statistical features from KNN classifier owing to it depends on calibration dataset. Also, when comparing the performance results of Fine KNN to previous studies, the classification accuracy also enhanced by 1.2%, sensitivity by 4.5%, and specificity by 2.7% over the largest one [7]. Because of the number of statistical features have been increased and the well-isolating technique have been used. Thanks to this study the medical professionals can be differentiated among DF cases accurately and can be presented in polyclinics as an aided tool to help them to validate their decision about a plantar foot. In the future, we propose to use more subjects in each group and classify the system by using deep learning algorithm without extracting features [9]. There will be the probability of establishing a mobile application also for the automatic diagnosis of the diabetic foot using thermal images which could be widely used in hospitals.

REFERENCES

[1] C. Liu, F. van der Heijden, M. E. Klein, J. G. van Baal, S. A. Bus, and J. J. van Netten, "Infrared dermal thermography on diabetic feet soles to predict ulcerations: a case study." p. 85720N.

[2] L. Fraiwan, M. AlKhodari, J. Ninan, B. Mustafa, A. Saleh, and M. Ghazal, "Diabetic foot ulcer mobile detection system using smart phone thermal camera: a feasibility study," *Biomedical engineering online*, vol. 16, no. 1, pp. 117, 2017.

[3] P.-C. Sun, S.-H. E. Jao, and C.-K. Cheng, "Assessing foot temperature using infrared thermography," *Foot & ankle international*, vol. 26, no. 10, pp. 847-853, 2005.

[4] G. Serbu, "Infrared imaging of the diabetic foot," *InfraMation Proc*, vol. 86, pp. 5-20, 2009.

[5] J. J. van Netten, J. G. van Baal, C. Liu, F. van Der Heijden, and S. A. Bus, "Infrared thermal imaging for automated detection of diabetic foot complications," SAGE Publications Sage CA: Los Angeles, CA, 2013.

[6] H. Peregrina-Barreto, L. A. Morales-Hernandez, J. Rangel-Magdaleno, J. G. Avina-Cervantes, J. M. Ramirez-Cortes, and R. Morales-Caporal, "Quantitative estimation of temperature variations in plantar angiosomes: a study case for diabetic foot," *Computational and mathematical methods in medicine*, vol. 2014, 2014.

[7] P. s, S. Angelin.P, Priyanka.R, Subasri.G, and Venkatesh.R, "Automated Detection of Diabetic Foot Using Thermal Images by Neural Network Classifiers," *International Journal of Emerging Trends in Science and Technology*, vol. 04, no. 05, pp. 6, 2017.

[8] K. Roback, "An overview of temperature monitoring devices for early detection of diabetic foot disorders," *Expert review of medical devices*, vol. 7, no. 5, pp. 711-718, 2010.

[9] M. Goyal, N. D. Reeves, A. K. Davison, S. Rajbhandari, J. Spragg, and M. H. Yap, "Dfunet: Convolutional neural networks for diabetic foot ulcer classification," *arXiv preprint arXiv:1711.10448*, 2017.

[10] M. Adam, E. Y. Ng, S. L. Oh, M. L. Heng, Y. Hagiwara, J. H. Tan, J. W. Tong, and U. R. Acharya, "Automated characterization of diabetic foot using nonlinear features extracted from thermograms," *Infrared Physics & Technology*, vol. 89, pp. 325-337, 2018.

[11] J. Yousefi, "Image Binarization using Otsu Thresholding Algorithm," 2011.

[12] R. C. Gonzalez, R. Woods, and S. Eddins, "Morphological reconstruction from digital image processing using MATLAB," *MATLAB Digest–Academic Edition*, 2008.

[13] M. Airouche, L. Bentabet, and M. Zelmat, "Image segmentation using active contour model and level set method applied to detect oil spills." pp. 1-3.

[14] A. Raid, W. Khedr, M. El-Dosuky, and M. Aoud, "Image restoration based on morphological operations," *International Journal of Computer Science, Engineering and Information Technology*, vol. 4, no. 3, pp. 9-21, 2014.

[15] A. E. Minarno, Y. Munarko, A. Kurniawardhani, F. Bimantoro, and N. Suciati, "Texture feature extraction using co-occurrence matrices of sub-band image for batik image classification." pp. 249-254.

[16] S. Sergyan, "Color histogram features based image classification in content-based image retrieval systems." pp. 221-224.

[17] M. Sharma, "A review: image fusion techniques and applications," *Int J Comput Sci Inf Technol*, vol. 7, no. 3, pp. 1082-1085, 2016.

[18] P. Thanh Noi, and M. Kappas, "Comparison of random forest, k-nearest neighbor, and support vector machine classifiers for land cover classification using Sentinel-2 imagery," *Sensors*, vol. 18, no. 1, pp. 18, 2017.

[19] R. Entezari-Maleki, A. Rezaei, and B. Minaei-Bidgoli, "Comparison of classification methods based on the type of attributes and sample size," *Journal of Convergence Information Technology*, vol. 4, no. 3, pp. 94-102, 2009.

[20] A. Ben-Hur, and J. Weston, "A user's guide to support vector machines," *Data mining techniques for the life sciences*, pp. 223-239: Springer, 2010.

[21] M. Hossin, and M. Sulaiman, "A review on evaluation metrics for data classification evaluations," *International Journal of Data Mining & Knowledge Management Process*, vol. 5, no. 2, pp. 1, 2015.

[22] T. Tamaki, "Screening for osteomyelitis using thermography in patients with diabetic foot," Ulcers, vol. 2013, 2013.

[23] J. J. van Netten, M. Prijs, J. G. van Baal, C. Liu, F. van Der Heijden, and S. A. Bus, "Diagnostic values for skin temperature assessment to detect diabetes-related foot complications," Diabetes technology & therapeutics, vol. 16, no. 11, pp. 714-721, 2014.

[24] D. Hernandez-Contreras, H. Peregrina-Barreto, J. Rangel-Magdaleno, J. Ramirez-Cortes, F. Renero-Carrillo, and G. Avina-Cervantes, "Evaluation of thermal patterns and distribution applied to the study of diabetic foot." pp. 482-487.

[25] R. Vardasca, L. Vaz, C. Magalhães, A. Seixas, and J. Mendes, "Towards the Diabetic Foot Ulcers Classification with Infrared Thermal Images."